SCIENCE CHINA
Earth Sciences

•RESEARCH PAPER•

July 2019 Vol.62 No.7: 1125–1137
https://doi.org/10.1007/s11430-018-9333-x

Increased winter-spring precipitation from the last glaciation to the Holocene inferred from a $\delta^{13}C_{org}$ record from Yili Basin (Xinjiang, NW China)

Keliang ZHAO[1,2*], Xiaoqiang LI[1,2†], Hai XU[3], Xingying ZHOU[1,2], John DODSON[4,5] & Junchi LIU[1]

[1] *Key Laboratory of Vertebrate Evolution and Human Origins, Institute of Vertebrate Paleontology and Paleoanthropology, Chinese Academy of Sciences, Beijing 100044, China;*
[2] *CAS Center for Excellence in Life and Paleoenvironment, Beijing 100044, China;*
[3] *Institute of Surface-Earth System Science, Tianjin University, Tianjing 300072, China;*
[4] *School of Earth, Atmospheric and Life Sciences, University of Wollongong, NSW 2522, Australia;*
[5] *Institute of Earth Environment, Chinese Academy of Sciences, Xi'an 710061, China*

Received September 7, 2018; revised November 24, 2018; accepted January 23, 2019; published online March 21, 2019

Abstract The nature and dynamics of climate change in central Asia since the late Pleistocene are controversial. Moreover, most of the published studies focus mainly on the evolution of moisture conditions, and there have been few attempts to address changes in seasonality. In this study, records of $\delta^{13}C_{org}$, TOC, TN, C/N and grain size were obtained from lacustrine sediments at Yili Basin, Xinjiang, NW China. Our aim was to reconstruct the trend in seasonality of precipitation from the last glaciation to the Holocene. The organic matter content of the sediments is derived predominantly from terrestrial plants. The $\delta^{13}C_{org}$ values vary from −19.4‰ to −24.8‰, indicating that the vegetation was dominated by C_3 plants. Winter-spring precipitation is identified as the factor determining the relative proportions of C_3 and C_4 plants in the region. A negative trend in $\delta^{13}C_{org}$ corresponding to an increase in the relative abundance of C_3 plants indicate a trend of increasing winter-spring precipitation from the last glaciation to the Holocene. The increased incidence of wintertime storms in the interior of Asia is suggested to result in the increase of winter-spring precipitation in the Holocene.

Keywords Organic matter, Central Asia, C_3 and C_4 plants, Seasonality changes, Winter-spring precipitation

Citation: Zhao K, Li X, Xu H, Zhou X, Dodson J, Liu J. 2019. Increased winter-spring precipitation from the last glaciation to the Holocene inferred from a $\delta^{13}C_{org}$ record from Yili Basin (Xinjiang, NW China). Science China Earth Sciences, 62: 1125–1137, https://doi.org/10.1007/s11430-018-9333-x

1. Introduction

The origin and evolution of the arid environment in central Asia, which includes the largest temperate arid zone in the world, is an important scientific issue within global climate change research programs (Rea et al., 1998; Guo et al., 2002; Sun et al., 2010; Liu et al., 2014; Zheng et al., 2015). Over the past several decades, late Pleistocene and Holocene climate changes within central Asia have been studied extensively, based on a variety of proxies and depositional contexts, including lacustrine sediments (e.g., Sun et al., 1994; Chen et al., 2008; Liu et al., 2008; Huang et al., 2009; Rudaya et al., 2009; Li et al., 2011; Rudaya and Li, 2013; Mathis et al., 2014; Zhang et al., 2016), loess deposits (e.g., Ye, 1999; Fang et al., 2002; Song et al., 2010; Rao et al., 2013; Ran and Feng, 2014), stalagmites (e.g., Cheng et al., 2012; Cai et al., 2017), and eolian dune sequences (e.g., Yang

* Corresponding author (email: zhaokeliang@ivpp.ac.cn)
† Corresponding author (email: lixiaoqiang@ivpp.ac.cn)

et al., 2002; Long et al., 2014, 2017). However, most of the published studies focus on the evolution of moisture conditions and relatively few studies have considered seasonality changes in central Asia since the late Pleistocene (Herzschuh, 2006; Yang and Ding, 2006; Kutzbach et al., 2013; Hong et al., 2014; Chen et al., 2016; Zhao et al., 2017).

There have been many studies of seasonality changes in the Northern Hemisphere (NH), and increased seasonality has been observed from the Pliocene to the Pleistocene (Haug et al., 2005; Hennissen et al., 2015). The winter-spring precipitation is the principal control on predominance of C_3 plants in central Asia over the past 1.77 Myr (Yang and Ding, 2006). Both climate models and paleoclimate records have reconstructed the moisture conditions in parts of the Mediterranean, the Middle East, and the interior of Asia, at times of maximum NH seasonality (summer perihelion-increased insolation; winter aphelion-decreased insolation) (Kutzbach et al., 2013). From 15 to 4 cal kyr BP, winter precipitation in the Mediterranean region was highest during warm intervals and lowest during cooling phases (Dormoy et al., 2009). These studies of seasonality changes provide new insights into the causes of apparent discrepancies between published paleoclimatic reconstructions based on pollen analysis, lake-levels and stable isotopes in several regions (Peyron et al., 2011).

Organic matter (OM) is a minor but important component of lacustrine sediments (Meyers and Lallier-Vergés, 1999). The carbon isotopic composition of OM ($\delta^{13}C_{org}$) has been extensively used to reconstruct the source vegetation (Meyers and Ishiwatari, 1993), CO_2 concentration (Meyers and Horie, 1993), paleoclimate (Gouveia et al., 2002; Mackay et al., 2012), and lake level history (Liu et al., 2013). It is generally considered that different sources of OM have different $\delta^{13}C_{org}$ signatures (Meyers and Lallier-Vergés, 1999). There are two major sources of lake OM: terrestrial plants (e.g., trees, shrubs, grasses) and aquatic plants (e.g., phytoplankton) (Meyers, 2003).

Terrestrial higher plants use two fundamentally different pathways of CO_2 fixation: the C_3 (Calvin-Benson) and C_4 (Hatch-Slack) cycles (Deines, 1980). C_3 plants, which include nearly all tree and most shrub and herb taxa, have $\delta^{13}C_{org}$ values from –32‰ to –22‰ with a mean of about –27‰; C_4 plants are mainly herbs and some shrubs, and have $\delta^{13}C_{org}$ values from –19‰ to –9‰, with an average of –13‰ (Deines, 1980; O'Leary, 1981; Farquhar et al., 1989). The competitive advantage difference between C_3 and C_4 plants is favored by environmental differences: C_3 plants prefer a cool growing season with an overall humid climate and high atmospheric CO_2 concentration, while C_4 plants have a competitive growth advantage under a scenario of warm-season precipitation and lower low atmospheric CO_2 concentration (Deines, 1980; O'Leary, 1981, 1988; Farquhar et al., 1989; Sage et al., 1999). Therefore, the $\delta^{13}C_{org}$ values of the organic fraction of lacustrine sediments, which is contributed mainly by terrestrial plants, should reflect the environmental response of different plants types (e.g. C_3 and C_4) and can be used to reconstruct the history of vegetation and hence paleoclimate (Giresse et al., 1994; Huang et al., 2001).

Yili Basin (also known as Ili Basin) is in the western Tien Shan Mountains, which has a wetter climate than most of central Asia (Figure 1). The modern climate is dominated by the mid-latitude westerlies with abundant lacustrine and loess sediment sequences which makes the region well suited for assessing climatic changes in central Asia. Li et al. (2011) and Zhao et al. (2013) reported a pollen record from a 12.2-m-long lacustrine sediment sequence, with robust dating control, from Yili Basin. The present study utilizes the

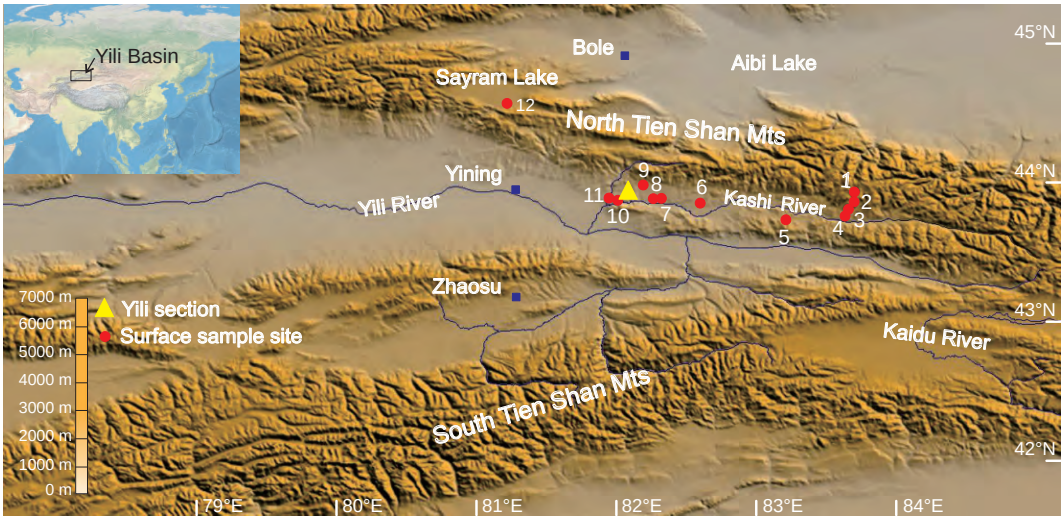

Figure 1 Location of Yili Basin and the study site. The yellow triangle indicates the position of Yili section; the red circle indicates the surface sample sites for $\delta^{13}C_{org}$ in the basin.

$\delta^{13}C_{org}$ records from the same sedimentary sequence with the aim of reconstructing the regional history of C_3/C_4 relative abundance and to detect regional changes in seasonality precipitation (e.g. the changes of winter-spring precipitation) from the late Pleistocene to the Holocene.

2. Study area

The Yili Basin is surrounded by the Tien Shan Mountains to the north, south and east (Figure 1). It has a temperate semi-arid continental climate and westerly winds prevail throughout the year. The moisture from the North Atlantic Ocean, Mediterranean, Black Seas and Aral-Caspian Basin play an important role on the precipitation in the area (Aizen et al., 2006; Böhner, 2006). Topography has a large influence on the mean annual temperature (MAT) and mean annual precipitation (MAP) of the region. MAT ranges from 2.6–10.4°C, while MAP ranges from 200–500 mm, between the basin plains and mountain areas (Li, 1991). The vegetation zones of the Yili Basin are altitudinally controlled and classified in descending order, as follows: alpine cushion-like vegetation, alpine meadow, montane forest-meadow, subalpine meadow, montane steppe and desert (Xinjiang Expedition Team, 1978) (Figure 2).

Yining (43°57′N, 81°20′E, 663 masl (meter above sea level)) and Zhaosu (43°09′N, 81°08′E, 1855 masl) are selected to represent the respective climatic characteristics of the plain and mountain areas of Yili Basin. As shown in Figure 3, the temperatures in Yining and Zhaosu exhibit the same trend from January to December, with maximum temperature occurring in July and minimum temperature in January. How-

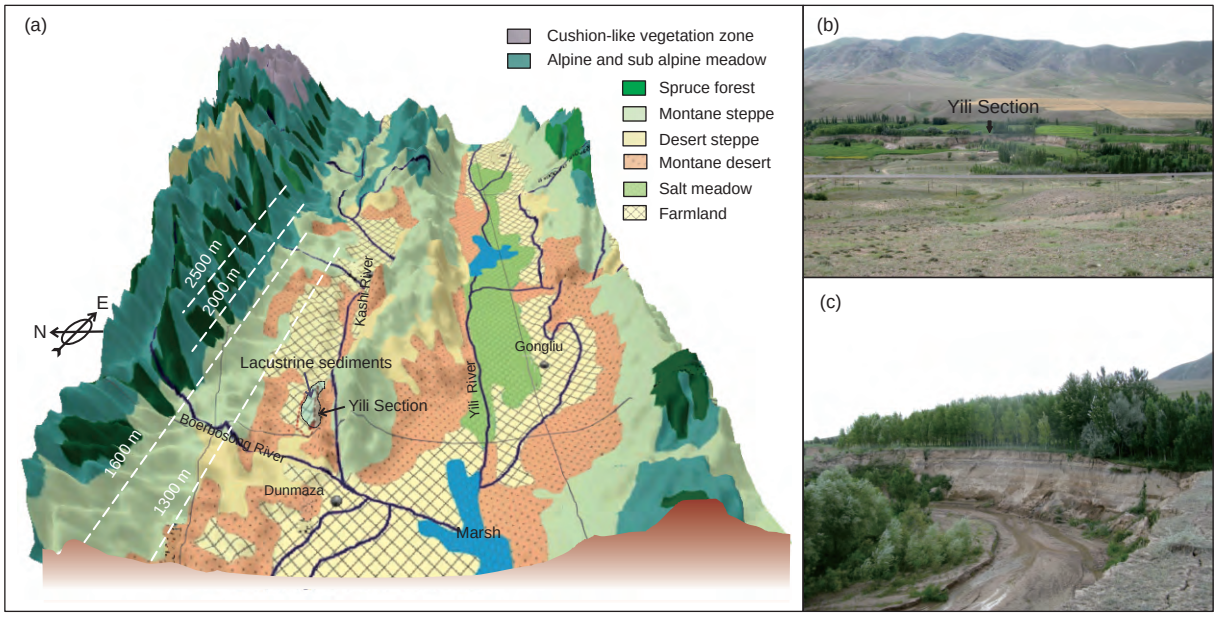

Figure 2 Vertical vegetation zones around the study site in the Yili Basin (a), long shot (b) and close-up (c) of the Yili section.

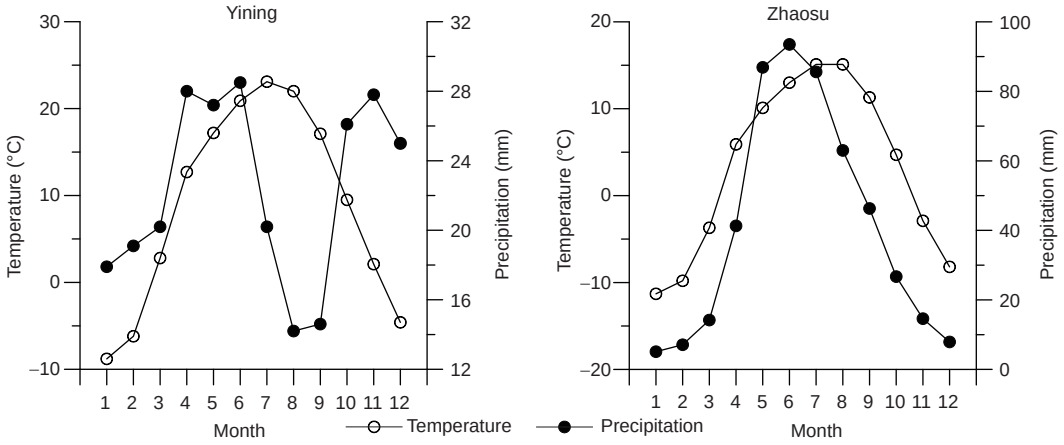

Figure 3 Variation of monthly mean temperature and precipitation in Yining and Zhaosu (average values from 1971 to 2000).

ever, the distributions of monthly mean precipitation are different; precipitation exhibits a double peak in Yining (May–June and October–December) and a single peak in Zhaosu (May–July) (Figure 3). The precipitation distributions in spring (March, April and May), summer (June, July and August), autumn (September, October and November) and winter (December, January and February) for both sites are listed in Table 1. The seasonal maximum precipitation occurs in spring in Yining, while the seasonal maximum precipitation occurs in summer in Zhaosu. However, a common characteristic of the two locations is that higher precipitation corresponds to temperatures in the range of 10–20°C.

3. Materials and methods

3.1 Sediments and dating

The Yili section (43°51′25.7″N, 81°57′54.3″E; 928 masl), a 12.2-m-deep sedimentary profile, is in an intramountain basin near Maza town, Yining City, Xinjiang Province (Figures 1 and 2). The section has clear horizontal bedding (Figures 2c and 4). A detailed description of the profile, as well as the chronological framework, has been published elsewhere (Li et al., 2011; Zhao et al., 2013) and therefore only basic information is given here. A total of 244 sediment samples were collected at 0.05-m intervals through the section. Eight charcoal samples and three shell samples were selected for AMS ^{14}C dating (Li et al., 2011; Zhao et al., 2013). Sample pretreatment and measurements were carried out at the Australian Nuclear Science and Technology Organization, Australia. Radiocarbon dates were converted to calibrated ages (2σ) following the procedure of Reimer et al. (2013) (Figure 4).

An age inversion occurs in the sample from 0.82–0.84 m, suggesting that the loess in the upper 1 m was disturbed (Figure 4). The present study focuses on the sediments from 1.1–12.2 m depth which are mainly composed of silts, sands and clays. Age-depth model for the interval from 1.1–8.9 m which was produced by the Bacon software package (Blaauw and Christen, 2011). An AMS ^{14}C date on a shell collected at 9.58–9.6 m depth is 30,964–31,493 cal yr BP, which falls within the last glaciation. According to the ages of the depths of 8.9 and 9.6 m and the interval of sandy sediment from 8.65–8.9 m, we conclude that a sedimentary hiatus occurs around the depth of 8.9 m, which may correspond to the Last

Table 1 Seasonal distribution of modern precipitation (mm) in Yining and Zhaosu

Site	Altitude (m)	Spring	Summer	Autumn	Winter	MAP
Yining	663	75	63	69	62	269
Zhaosu	1855	142	242	88	20	492

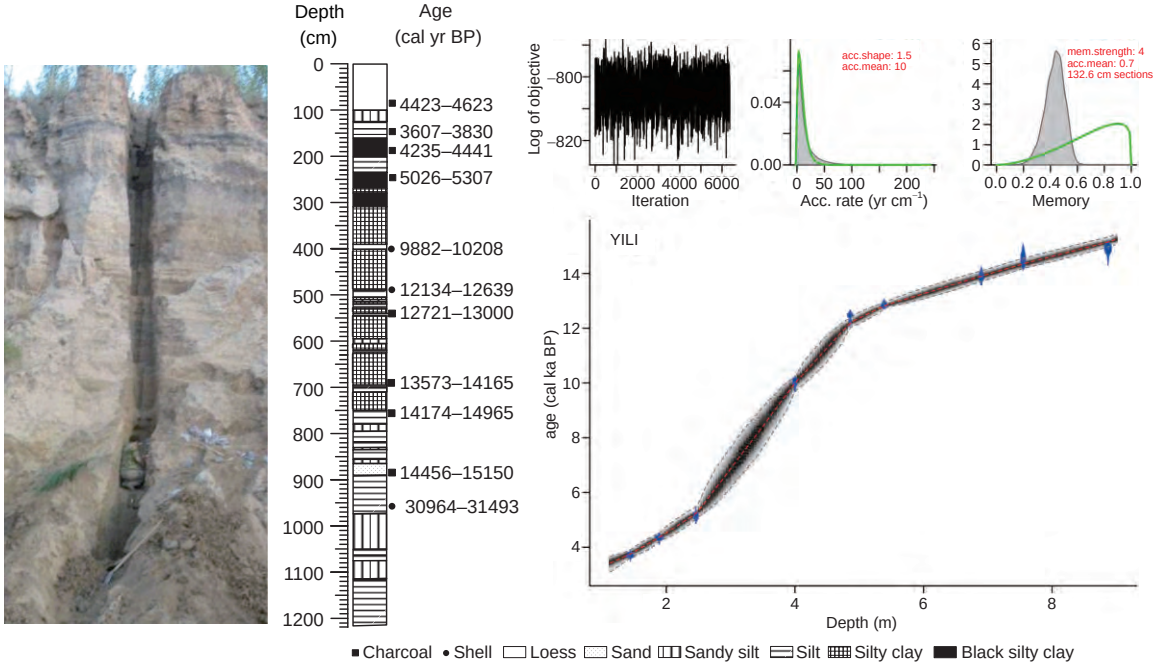

Figure 4 Age-depth model for Yili section produced by the Bacon software package (Blaauw and Christen, 2011). AMS^{14}C ages were calibrated with the IntCal13 curve (2σ) (Reimer et al., 2013).

Glacial Maximum (LGM) (Zhao et al., 2013). The Bacon model isn't used below 8.9 m because of the hiatus and different lithology with the depth of 1.1–8.9 m.

3.2 Surface soil samples

Twelve surface soil samples (at the depth of 0–0.02 m) were collected from different vegetation communities in the Yili Basin (Figure 1, red circle), including one sample from Cupressaceae shrubland, one from a *Picea schrenkiana* forest, two from subalpine meadows, two from montane steppe, three from *Artemisia* desert, one from a *Populus euphratica* forest and one from a Chenopodiaceae desert shrubland. Within each vegetation community, the samples were collected from randomly selected plots. The surface soil $\delta^{13}C_{org}$ values were measured to provide a basis for interpreting the $\delta^{13}C_{org}$ record from the lacustrine sediments.

3.3 Measurements of $\delta^{13}C_{org}$, TOC, TN, and grain size

A total of 111 sediment samples (from 1.1–12.2 m depth in the section) and 12 surface soil samples were analyzed for $\delta^{13}C_{org}$. The samples were oven-dried at 40°C for 24 h, ground in an agate mortar after removing modern rootlets with the aid of a stereomicroscope, and sieved through a 100 μm mesh and homogenized. Approximately 3 g of each sieved sediment sample was treated with 2 mol L^{-1} HCL at room temperature to remove carbonates, then rinsed to a pH of 7 with deionized water and dried at 40°C.

All the dried samples were combusted for 4 h at 850°C in evacuated sealed quartz tubes in the presence of 1 g of CuO, 1 g of Cu and Pt foil. The carbon dioxide was then cryogenically purified. The isotopic ratios of the purified CO_2 were measured using a Finnigan MAT 251 gas source mass spectrometer at the Institute of Earth Environment, Chinese Academy of Sciences (Liu et al, 2005a). Isotopic ratios are reported using δ-notation in per mil (‰) relative to the V-PDB standard for C. We used a Chinese National Standard reference material GBW04407 ($\delta^{13}C_{GBW04407/VPDB}$=–22.43‰ ±0.07‰) and an international isotope reference material USGS24 ($\delta^{13}C_{USGS24/VPDB}$=–16.049‰±0.035‰) to control the overall precision of the analyses. The overall precision of the $\delta^{13}C_{org}$ analysis was better than 0.2‰ with an average of 0.13‰. 85 dried samples were selected for total organic carbon (TOC) and total nitrogen (TN) measurements using an elemental analyzer (Costech ECS 4024) with a combustion temperature of 980°C at the Institute of Vertebrate Paleontology and Paleoanthropology, Chinese Academy of Sciences. The TOC and TN were used to calculate TOC/TN (C/N) ratios.

The grain-size distributions of 220 samples from 1.1–12.2 m depth were analyzed using a Mastersizer 2000 laser analyser with a measurement range of 0.02–2000 μm at the Institute of Earth Environment, Chinese Academy of Sciences. Samples weighing 2 g were pretreated with 15 mL 10% H_2O_2 to remove OM and then with 10 mL of warm 10% HCl to remove carbonates. Deionized water was added to remove acidic ions. The sample residue was finally treated with 10 mL of 0.05 mol L^{-1} $(NaPO_3)_6$ on an ultrasonic vibrator for 10 min to facilitate dispersion before grain-size analysis. The mean grain size (MGS) value is reported in this study.

3.4 Calculation of C_3/C_4 plant abundance and the end-members

Soil $\delta^{13}C_{org}$, an effective indicator of C_3/C_4 relative abundance, which has been used widely to reconstruct paleovegetation and paleoclimate (Meyers and Lallier-Vergés, 1999; Liu et al., 2005a; Rao et al., 2010; Yang et al., 2015). For calculation of C_3/C_4 plant abundance, the following mass balance equations are used:

$$C_3(\%)=(\delta^{13}C_{org}-\delta^{13}C_{C_4})/(\delta^{13}C_{C_3}-\delta^{13}C_{C_4})\times 100, \quad (1)$$

$$C_4(\%)=100-C_3(\%), \quad (2)$$

where C_3 (%) and C_4 (%) are percentages of C_3 and C_4 abundance in the local vegetation; $\delta^{13}C_{C_3}$ and $\delta^{13}C_{C_4}$ are the respective end-member values for C_3 and C_4 plants at a given locality and time of the soil deposit. The end-member values are impacted by many factors, such as temperature, precipitation, atmospheric CO_2 concentration, $\delta^{13}C_{org}$ of atmospheric CO_2 ($\delta^{13}C_{atm}$) and pedogenesis (Balesdent et al., 1993; Buchmann et al., 1997; Wang et al., 2008).

With reference to the studies of vegetation and loess soil $\delta^{13}C_{org}$ values in China, Tajikistan and Kazakhstan (Gu et al., 2003; Yang and Ding, 2006; Wang et al., 2008; Rao et al., 2010; Ran and Feng, 2014; Yang et al., 2015), we assume that –26.7‰ and –12.8‰ for the end-member values of modern C_3 and C_4 plants. The $\delta^{13}C_{C_3}$ and $\delta^{13}C_{C_4}$ values then are obtained in view of the effect of $\delta^{13}C_{atm}$ and degradation in different phases (Appendix Table S1, https://link.springer.com). The effect of changes in temperature, precipitation, atmospheric CO_2 concentration are neglected because the relationship between these factors and $\delta^{13}C_{org}$ of plants in the Yili Basin is unknown. The proportions of C_3 and C_4 plants should be regarded as estimates because the end-members of $\delta^{13}C_{org}$ are not known precisely, varying slightly in response to environmental and genetic variations (Nordt et al., 2002; Wynn, 2007).

4. Results

4.1 Surface soil $\delta^{13}C_{org}$ data and C_3/C_4 relative abundance

The twelve surface soil $\delta^{13}C_{org}$ values range from –28.8‰ to

–23.9‰ with an average of –25.3‰ (Table 2). The most positive $\delta^{13}C_{org}$ value occurs in mountain steppe (–23.9‰) dominated by Poaceae and *Artemisia*, while the most negative value is from *Populus euphratica* forest (–28.8‰). The $\delta^{13}C_{org}$ values from *Picea schrenkiana* forest (–27.2‰) and *Populus euphratica* forest are more negative than those from Cupressaceae shrubland, *Artemisia* desert, Chenopodiaceae desert, mountain steppe and subalpine meadow.

According to the results obtained using mass balance eqs. (1) and (2), the surface soil $\delta^{13}C_{org}$ values indicate that the C_3 and C_4 plant average abundances are about 94.6% and 5.4% in the region (Table 2). That is the modern vegetation in the basin is dominated by C_3 plants. The C_3 plant abundance is high in *Picea schrenkiana* forest, *Populus euphratica* forest, subalpine meadow. A minor C_4 plant signal is observed in mountain steppe, Chenopodiceae desert and *Artemisia* desert, possibly because C_4 species are better represented within the Chenopodiaceae and Poaceae.

There are no published records of the modern distribution of C_3 and C_4 plants in the Yili Basin, but many studies have been carried out within the surrounding regions in Xinjiang. An investigation of the $\delta^{13}C_{org}$ values of 35 plant species in Aibi Lake Wetland located north of Yili Basin revealed 31 C_3 and 4 C_4 plant species respectively (He et al., 2010). An analysis of the $\delta^{13}C_{org}$ values of 53 plant species in the southern margin of the Junggar Basin showed that 34 species were C_3 plants and 19 species were C_4 plants (Chen et al., 2002; Sun et al., 2007).

There are more than 4000 native plant species in Xinjiang and they are predominantly C_3 plants. C_4 plants are favored by the arid, saline and alluvial fan fringe areas in Xinjiang. Fourteen families, 63 genera and 279 species of C_4 plants are known from the desert areas of Xinjiang, of which 110 are species of Chenopodiaceae, 32 Poaceae, 27 Cyperaceae, 27 Liliaceae, and 25 Polygonaceae (Feng et al., 2012). The relative abundance of C_4 (5.4%) plants in Yili Basin calculated using eqs. (1) and (2) is close to the average C_4 abundance (279/4000) in the Xinjiang area. It means the end-members are effective, and can be used to reconstruct the C_3 and C_4 abundance in the sediment.

4.2 TOC, TN and C/N

TOC varies from 0.05–2.17% with an average of 0.39% (Figure 5e), and TN from 0.01–0.15% with an average of 0.03% (Figure 5f). The TOC values of most of the samples are less than 0.3%, while the TN values are ~0.02 from 12.2–7.6 m; above 7.6 m (14.4 cal kyr BP), the TN values rise gradually. The highest TOC and TN values occur within the depth interval of 1.7–1.75 m (4.1 cal kyr BP). The TOC in 64.7% of the samples is < 0.3%, and the TN in 52.9% of the samples ranges from 0.01–0.02. The C/N ratios range from 5–22 with average of 10.6 (Figure 5g); the maximum value occurs at the depth of 10.2 m and the minimum at 8.8 m.

4.3 $\delta^{13}C_{org}$ and grain size record of the Yili section

The $\delta^{13}C_{org}$ values of the Yili section (Figure 5c) range between –19.4‰ and –24.8‰ with an average of –22.3‰. The $\delta^{13}C_{org}$ values are more positive, with an average of –20.7‰, within the depth interval of 12.2–9 m, corresponding to the time of last glaciation. The average value decreases to –21.1‰ at the depth of 8.9–7.6 m (15.2–14.4 cal kyr BP). The values become more negative (average of –23.3‰) from 7.6–1.1 m (14.1–3.4 cal kyr BP); they are relatively stable from 4.2–2.4 m (10.6–5.2 cal kyr BP), with an average of –23.9‰; and they fluctuate above 2.4 m depth (5.2 cal kyr

Table 2 Surface soil $\delta^{13}C_{org}$ values and C_3/C_4 abundance from Yili Basin

Sample site	$\delta^{13}C_{org}$ (‰)	Vegetation type	Altitude (m)	C_3 (%)	C_4 (%)
1	–24.8	Cupressaceae shrubs	2656	93.5	6.5
2	–27.2	*Picea schrenkiana* forest	2502	100	0
3	–25.8	Subalpine meadow	1926	100	0
4	–25.8	Subalpine meadow	1885	100	0
5	–24.1	Montane steppe	1576	88.5	11.5
6	–28.8	*Populus euphratica* forest	1173	100	0
7	–24.4	Chenopodiceae desert	1014	91.2	8.8
8	–23.9	*Artemisia* desert	1021	87.6	12.4
9	–25.7	*Artemisia* desert	1183	100	0
10	–23.9	Chenopodiceae desert	975	87.7	12.3
11	–25.5	*Artemisia* desert	1005	98.9	1.1
12	–23.9	Montane steppe	2136	87.2	12.8
Average value	–25.3			94.6	5.4

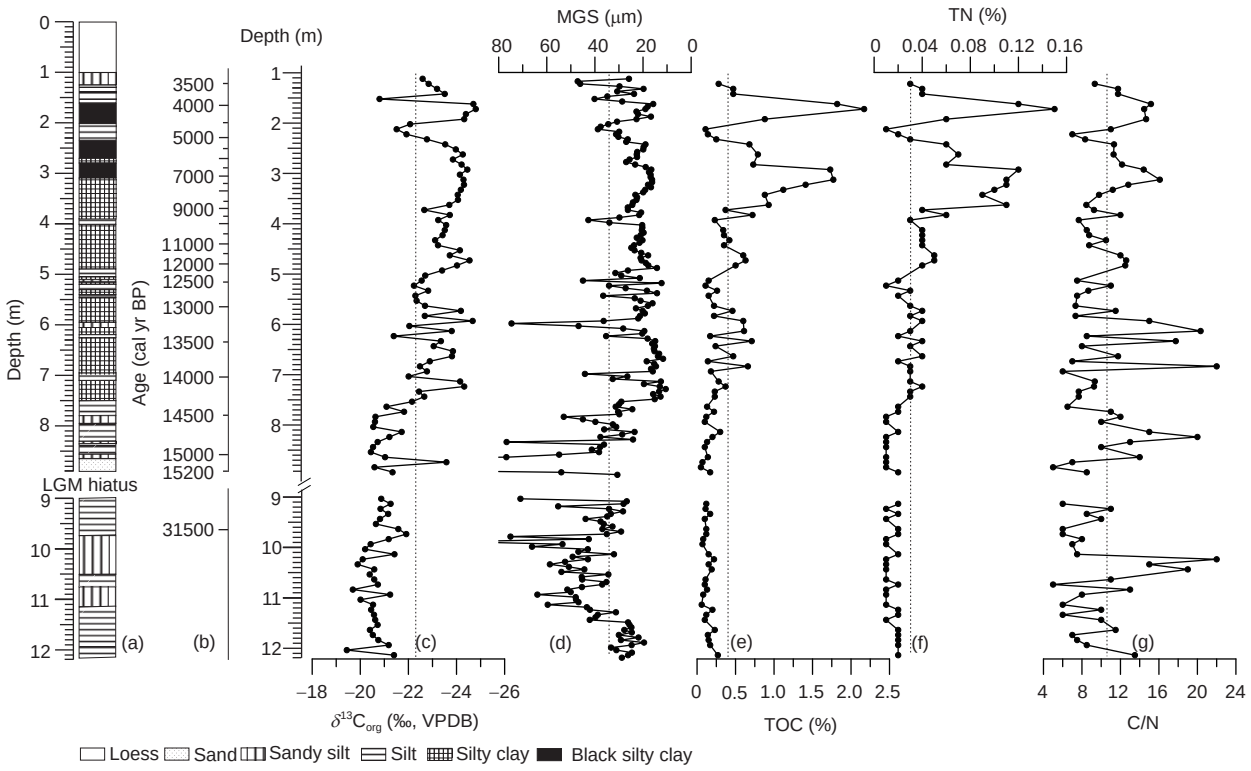

Figure 5 Lithology (a), age (b), $\delta^{13}C_{org}$ (c), mean grain size (MGS) (d), TOC (e), TN (f) and C/N ratio (g) for the Yili section. The dashed lines are the average values for specific intervals. In (d), MGS values ≥80 μm are clipped to the axis limits to highlight the major trends.

BP), with an average of –23.1‰. The maximum $\delta^{13}C_{org}$ value (–19.4‰) occurs at the depth of 12–12.05 m, while the minimum (–24.8‰) occurs at the depth of 1.7–1.75 m (4.1 cal kyr BP). Overall, there is a negative trend of $\delta^{13}C_{org}$ values from the late Pleistocene to the Holocene.

For the entire profile, the MGS varies from 10.6–245.3 μm with an average of 34.4 μm (Figure 5d), and there is an overall decreasing trend of MGS from the late Pleistocene to the Holocene. Within the depth interval of 12.2–8.9 m, the MGS ranges from 19.6–98.5 μm, with an average of 40.9 μm; from 8.9–7.6 m (15.2–14.4 cal kyr BP) it ranges from 23.5–245.3 μm, with an average of 69 μm; from 7.6–2.4 m (14.4–5.2 cal kyr BP), the average MGS decreases to 23.5 μm; and above 2.4 m (5.2 cal kyr BP), the MGS becomes more variable. In generally, the MGS values show a similar trend of variation to $\delta^{13}C_{org}$ records.

5. Discussion

5.1 Source of the sedimentary OM

Distinguishing the OM source of sediments is an important precondition for tracing climatic changes using $\delta^{13}C_{org}$ (Meyers and Lallier-Vergés, 1999). The OM of eolian sediment is derived from terrestrial vegetation growing around the site and very little is contributed by aquatic plants (Rao et al., 2013; Liu et al., 2005b). However, there are two sources of OM in lake sediments: from terrestrial and aquatic plants (Meyers and Lallier-Vergés, 1999). For example, the OM content of the sediments of Gucheng Lake (Shen et al., 1998a), Dabusu Lake (Shen et al., 1998b), Barkol Lake (Sun et al., 2014) and Lop Nur (Luo et al., 2008) is mainly of allochthonous origin from terrestrial vegetation, while in the case of Biwa Lake (Meyers and Horie, 1993), Wulungu Lake (Liu et al., 2008) the sources are mainly autochthonous, from aquatic plants.

In general, C/N ratios are an effective indicator for distinguishing the source of OM. C/N ratios <10 occur where the OM is dominated by aquatic plants which have a relatively high protein and low cellulose content; C/N ratios>10, and even >20, occur where the OM is dominated by terrestrial plants which have high content of vascular material and a low protein content (Meyers, 2003). However, the C/N ratio is unsuitable for inferring the source of OM in some shallow lakes because (1) the OM may be degraded due to stronger oxidizing conditions, and (2) the C/N ratios may be influenced by inorganic nitrogen, especially when the TOC content is <0.3% (Meyers, 2003; Woszczyk et al., 2011; Wang et al., 2012). Since the TOC content of most of the samples from the Yili section is <0.3%, the C/N is unsuitable for diagnosing the source of the OM.

In the interval before the last deglaciation, the MGS is coarser while the $\delta^{13}C_{org}$ values are more positive. After the last deglaciation, the grain size decreases, and the $\delta^{13}C_{org}$

values become more negative. The $\delta^{13}C_{org}$ values are positively correlated with the MGS within the section (Figure 6). The MGS reflects the strength of hydrodynamic conditions, which suggests that the $\delta^{13}C_{org}$ values are substantially or predominantly influenced by hydrodynamic conditions which promote the transport of terrigenous materials to the lake. The dry climate during the last glaciation led to lower lake levels, so the water flow can bring more coarse gain sizes to the site. During the last deglaciation and Holocene, the climate become wetter and the lake level rose, resulting in more finer grain sizes arriving at the site.

Pollen records can provide useful information about the origin of sedimentary OM (Giresse et al., 1994; Rudaya and Li, 2013). The pollen record of the Yili section indicates that since the late part of the last glaciation the vegetation at the site was dominated by herbs such as *Artemisia*, Chenopodiaceae, Poaceae and Compositae (Figure 7a) (Li et al., 2011; Zhao et al., 2013). The representation of aquatic plant pollen in the Yili section is very low and only exceeds 1% in a few samples. *Typha* representation is >1% in a single sample from the depth of 7.4–7.45 m, which is dominated by Chenopodiaceae (54.6%). The Sparganiaceae pollen content is >1% at the depth of 3.2–3.55 m, which is dominated by *Artemisia* (28.6%) and Compositae (30.8%) (Li et al., 2011). Therefore, it is clear that the OM content of the Yili section is predominantly derived from terrestrial plants (C_3 and C_4) around the site.

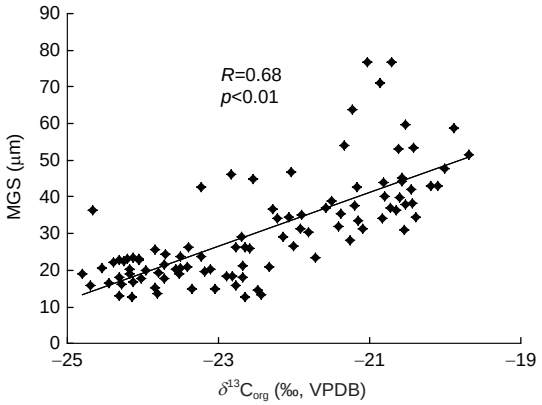

Figure 6 Scatter plot showing the relationship between mean grain size (MGS) and $\delta^{13}C_{org}$ for the Yili section. MGS values ≥80 μm are clipped in the figure.

5.2 Changes in C_3/C_4 relative abundance from the last glaciation to the Holocene

The mass balance eqs. (1) and (2) were used to calculate changes in the relative abundances of C_3 and C_4 plants since the last glaciation (Figure 7c). The average C_3 relative abundance is 73.3% at the depth of 12.2–9 m. At the beginning of the last deglaciation (8.9–7.6 m, 15.2–14.4 cal kyr

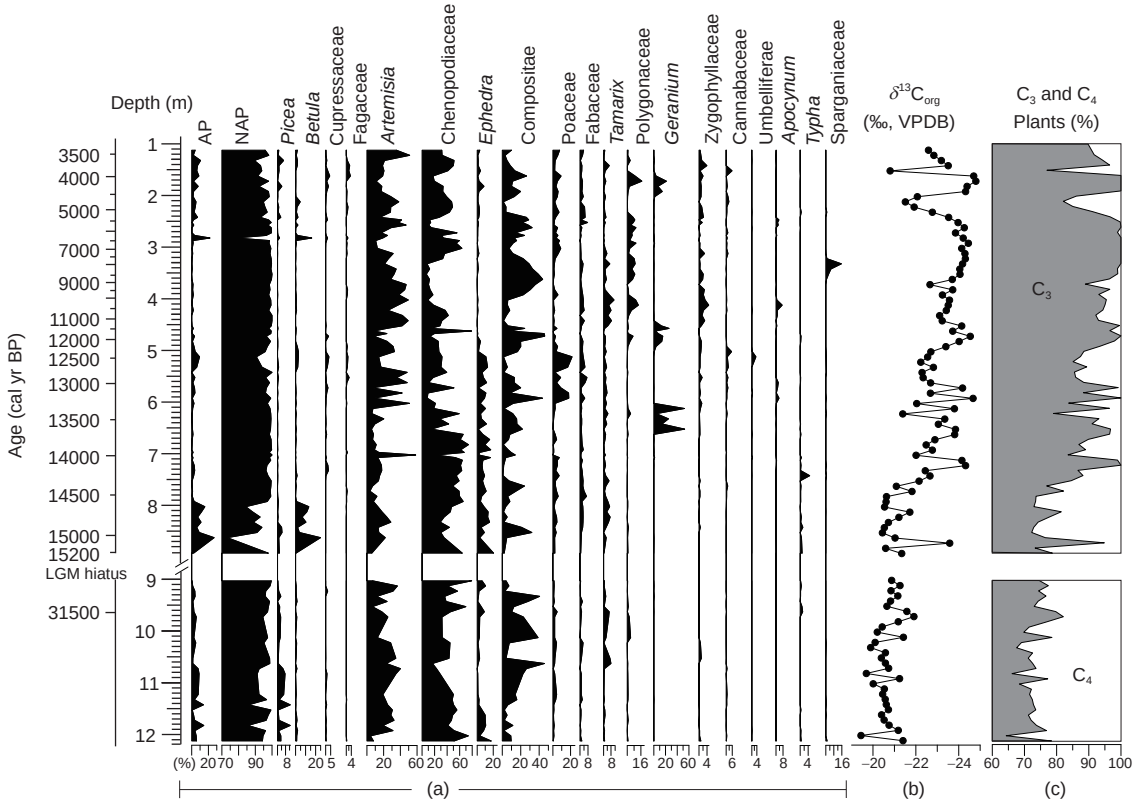

Figure 7 Pollen stratigraphy (a), $\delta^{13}C_{org}$ (b), calculate representation of C_3 and C_4 plants (c) for the Yili section.

BP), the C_3 proportion increased to 77.2%. The average C_3 proportion was up to 93.3% within the depth interval of 7.6–1.1 m (14.4–3.4 cal kyr BP). The C_3/C_4, relative abundance was unstable during 5.2–3.4 cal kyr BP.

The calculations indicate that from the last glaciation to the Holocene the local vegetation was dominated by C_3 plants, with an overall increasing trend of C_3 plant representation and a decreasing trend of C_4 plant representation (Figure 7c). We infer that C_3 representation was relatively low in the last glaciation and high during the deglaciation and Holocene, while the representation of C_4 plants exhibited the reverse trend.

More C_4 species are present the Chenopodiaceae and Poaceae families, thus we investigate the relationship between the two families and the C_4 biomass recovered in this study. There is a positive correlation (R=0.35, p<0.01) between Chenopodiaceae pollen proportion and C_4 (%) (Figure 8a). As shown in Figure 7, more C_4 (%) corresponds to high percentages of Chenopodiaceae pollen at the depth of 12.2–6.5 m, and less C_4 (%) corresponds to low Chenopodiaceae values at the depth of 6.5–1.1 m (13.6–3.4 cal kyr BP). We suggest that Chenopodiaceae species have a significant contribution to C_4 values in the sediment. There is a negative correlation between Poaceae pollen percentage and C_4 (%) (Figure 8b). Although it is difficult to distinguish the C_3 and C_4 types on the base of pollen morphology, the negative relationship is likely to mean that the Poaceae is dominated by C_3 types in the Yili Basin.

Our results are supported by $\delta^{13}C_{org}$ records from loess deposits from Tajikistan, Kazakhstan and the Yili Basin, which all indicate that the vegetation in central Asia was dominated by C_3 plants (Yang and Ding, 2006; Rao et al., 2013; Ran and Feng, 2014). A minor C_4 biomass peak occurred at ~228, 171 and 18 kyr BP when loess was deposited during cold and dry intervals in Tajikistan (Yang and Ding, 2006). The relative abundance of C_4 plants reached a maximum (~15%) during the cold LGM (~25–~19 kyr BP) in Kazakhstan (Ran and Feng, 2014). We conclude that the same mechanism was responsible for controlling the C_3/C_4 relative abundance in Central Asia.

5.3 Factors controlling C_3/C_4 relative abundance in the study area

Temperature, precipitation and CO_2 concentration are usually considered to be the main factors controlling the development of terrestrial vegetation, including C_3/C_4 relative abundance (O'Leary, 1988; Farquhar et al., 1989; Wang et al., 2014). Next, we compare our records of $\delta^{13}C_{org}$ and C_3/C_4 relative abundance from the Yili section with the $\delta^{18}O$ paleotemperature record from the GISP2 Greenland ice core (Stuiver et al., 1995; Grootes and Stuiver, 1997), a composite ice core record of pCO_2 from Antarctica (Petit et al., 1999; Monnin et al., 2001) and the $\delta^{18}O$ records from Kesang Cave stalagmite (Cheng et al., 2012) to consider the potential factors controlling local C_3/C_4 relative abundance.

It is currently assumed that the $\delta^{13}C_{org}$ values of C_3 plants become more positive with increasing temperature (Wang et al., 2013; Lu et al., 2015), and that C_4 plants also favour higher temperatures. If temperature is the dominant factor, $\delta^{13}C_{org}$ will become more positive, reflecting an increasing proportion of C_4 vegetation during the Holocene. However, our results for the Yili section show that the $\delta^{13}C_{org}$ values became more negative with increasing temperature, suggesting an increase in the relative abundance of C_3 plants (Figure 9a–9c). Therefore, we conclude that temperature change was not the dominant influence on changes in $\delta^{13}C_{org}$ and C_3/C_4 relative abundance in the study area.

An increase in CO_2 concentration favors C_3 plants which would potentially cause the $\delta^{13}C_{org}$ values of C_3 plants to become more negative (Schubert and Jahren, 2012; Wang et al., 2014). Our records show that $\delta^{13}C_{org}$ values became more negative, in accord with the increasing CO_2 concentration during the last deglaciation; however, this inverse relationship is not observed during the Holocene (Figure 9a and 9d). The $\delta^{13}C_{org}$ values vary and are more positive with the rise in CO_2 concentration from 5 cal kyr BP. The assumption of CO_2 control cannot explain the fluctuations in $\delta^{13}C_{org}$ values following about 5.2 kyr BP.

Despite the numerous glacial-interglacial cycles and associated fluctuations in temperature and CO_2 over past 1.77

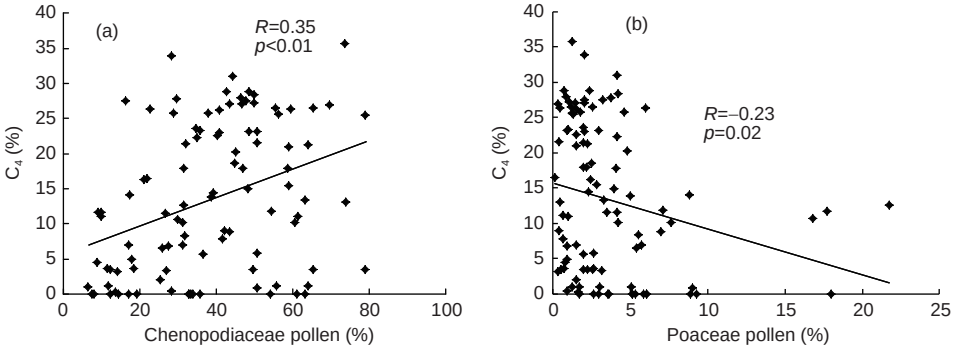

Figure 8 Scatter plot showing the relationship between C_4 biomass and Chenopodiaceae (a) and Poaceae (b) pollen percentages for the Yili section.

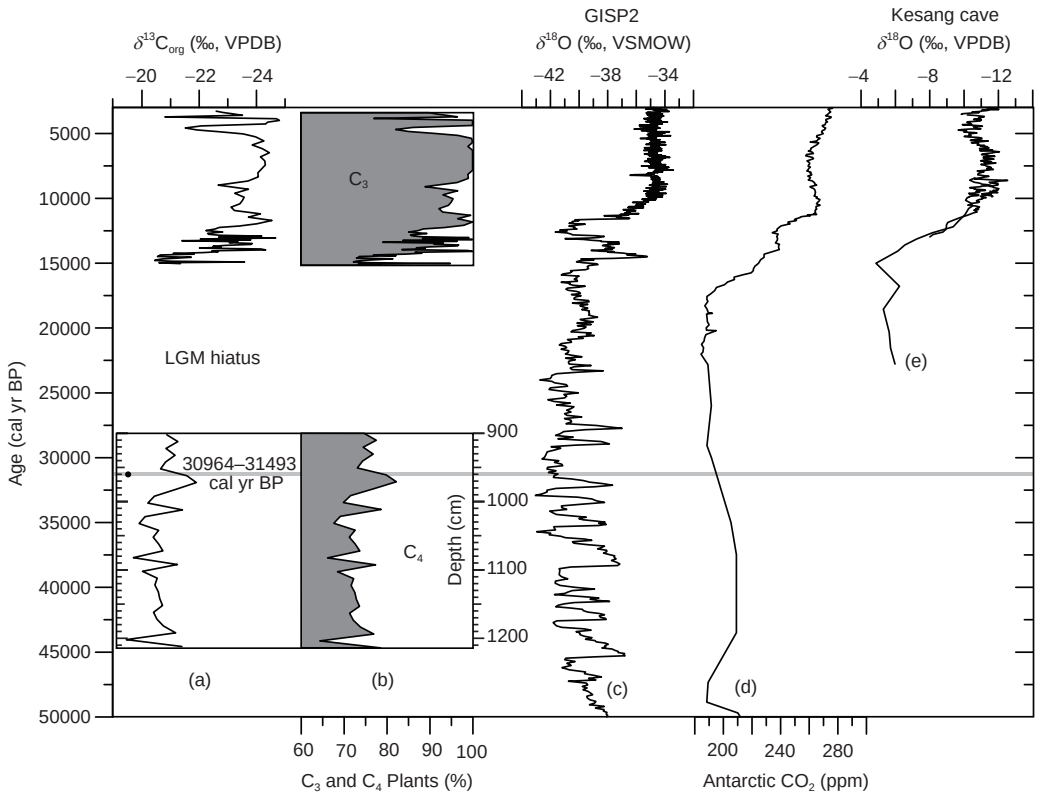

Figure 9 Comparison of records of $\delta^{13}C_{org}$ (a), C_3 and C_4 plant abundance (%) (b) in Yili Basin with the $\delta^{18}O$ paleotemperature record from the GISP2 Greenland ice core (c) (Stuiver et al., 1995; Grootes and Stuiver, 1997), a composite CO_2 record from Antarctica (d) (Petit et al., 1999, Monnin et al., 2001) and the $\delta^{18}O$ record from Kesang Cave (e) in Yili Basin (Cheng et al., 2012). 1 ppm=1 mg L^{-1}.

Myr, the vegetation remained continuously dominated by C_3 plants. Thus, temperature and CO_2 evidently had little influence on the C_3/C_4 relative abundance in central Asia (Yang and Ding, 2006). The $\delta^{13}C_{org}$ records from loess deposits in north China and from lake sediments in Central America (Huang et al., 2001; Lu et al., 2015) also suggest that CO_2 concentration was not the dominant factor influencing $\delta^{13}C_{org}$ changes. Therefore, we exclude that CO_2 concentration was the main driver of $\delta^{13}C_{org}$ changes in our records, and this conclusion is supported by studies of the $\delta^{13}C_{org}$ values of modern soils and vegetation (Lee et al., 2005; Rao et al., 2010; Wang et al., 2013).

Surface soil $\delta^{13}C_{org}$ values from arid and semi-arid areas in central East Asia were found to be negatively correlated with precipitation from May to September (Lee et al., 2005). The $\delta^{13}C_{org}$ values of loess sediments in the Yili Basin reflects the response of C_3 plants to changes in precipitation (Rao et al., 2013), while the $\delta^{13}C_{org}$ values of loess in Kazakhstan were used to reflect moisture changes in the area since ~46 kyr BP (Ran and Feng, 2014). The $\delta^{13}C_{org}$ values of loess in Tajikistan suggest that winter-spring precipitation was the principal factor causing the predominance of C_3 plants in central Asia over the past 1.77 Myr (Yang and Ding, 2006). We conclude that C_3/C_4 relative abundance in Yili Basin from the last glaciation to the Holocene was largely controlled by winter-spring precipitation. Increasing winter-spring precipitation resulted in an increase in C_3 relative abundances, and hence more negative $\delta^{13}C_{org}$ values in the study region.

The $\delta^{18}O$ records of stalagmite from Kesang Cave in Yili Valley demonstrates that the precipitation increased from last glaciation to the Holocene (Cheng et al., 2012) (Figure 9e). Arguably, increased MAP also was responsible for driving the $\delta^{13}C_{org}$ of C_3 plants towards more negative values from the last glaciation to the Holocene. However, if this were the case, the MAP would have increased by about 650 mm in the basin from the last glaciation (–20.7‰) to the Holocene (–23.3‰), based on the –0.40‰ change per 100 mm increase in MAP in north China (Wang et al., 2008). The modern MAP is ~269 mm, and the 650-mm increase means that there was almost no precipitation in the study region during the last glaciation. Our pollen and sediment data evidently do not support this conclusion (Zhao et al., 2013). The effect of MAP on negative trend of the C_3 plants $\delta^{13}C_{org}$ can be neglected. The seasonal rainfall played an important role in controlling C_3/C_4 plant relative abundance which dominated the $\delta^{13}C_{org}$ values changes.

The seasonality does change spatially from winter precipitation in the Eastern Mediterranean and the main part of central Asia to spring-summer precipitation in eastern central Asia (Cheng et al., 2012; Kutzbach et al., 2013). Yili Basin is

close to the boundary of the seasonality change and thus could be subject to temporal changes in seasonality. The winter-spring rainfall, especially the spring rainfall, can increase effective moisture to the soil because of more precipitation and relative low temperature (e.g. low evaporation). This benefits the growth of plants and results in the increased abundance of C_3 in the basin.

5.4 Origin of the increased winter-spring rainfall since the last deglaciation

The trend of decreasing $\delta^{13}C_{org}$ in the study section indicates a progressive increase in winter-spring rainfall from the last glaciation to the Holocene in the Yili Basin. Thus, winter-spring rainfall was greater in the warmer Holocene than during the colder last glaciation. Relatively high winter-spring rainfall (i.e. a Mediterranean-type climate), is one of the principal features of the modern distribution of seasonal precipitation in most of central Asia. However, the seasonal distribution pattern of precipitation during the last glaciation may have been different from that of today (i.e., with less winter-spring rainfall than today). Our conclusion is supported by other paleoclimatic records from the Mediterranean, the Middle East, and the interior of Asia (Peyron et al., 2011). In addition, most climate models simulate enhanced winter rainfall in the Mediterranean during the early to mid-Holocene (Hewitt and Mitchell, 1996). Moreover, pollen records reveal that winter precipitation was highest during warm intervals and lowest in cool intervals between 15 and 4 kyr BP in the Mediterranean region (Dormoy et al., 2009).

Climate model simulations indicate the wetter periods in the Mediterranean, the Middle East, and the interior of Asia, occurring at times of maximum NH seasonality, are linked to increased wintertime storm track precipitation, or a combination of increased winter and summer rainfall (Kutzbach et al., 2013). On the precession scale, NH summer coincided with perihelion at the beginning of the Holocene (11–10 kyr BP) and resulted in more winter-spring precipitation. Therefore, we attribute the increased winter-spring precipitation from the last glaciation to Holocene in Yili Basin to increased wintertime storms in the middle latitudes of Asia (Kutzbach et al., 2013).

6. Conclusions

We have used $\delta^{13}C_{org}$ records from Yili Basin in Xinjiang Province, China, to reconstruct past changes in C_3/C_4 relative abundance and corresponding climate changes in central Asia from the last glaciation to the Holocene. Our results show that the vegetation was dominated by C_3 plants since the last glaciation, while C_4 plants were slightly better represented in the last glaciation than in the Holocene. Based on comparisons with other paleoclimatic records, combined with climate simulations, we conclude that winter-spring precipitation was the dominant factor controlling C_3/C_4 relative abundance. The negative trend of $\delta^{13}C_{org}$ and increasing C_3 relative abundance indicate an increase in winter-spring precipitation from the last glaciation to the Holocene. We suggest that increasing wintertime storm tracks in central Asia were responsible for the trend of increasing winter-spring precipitation in the region.

Acknowledgements *We thank Dr. Guilin Zhang for helpful discussions about the age model. This study was supported by the Strategic Priority Research Program of Chinese Academy of Sciences (Grant No. XDB26000000), the National Natural Science Foundation of China (Grant Nos. 41772371, 41572161 & 41730319), the National Basic Research Program of China (Grant No. 2015CB953803), the Youth Innovation Promotion Association CAS, and the Australian Nuclear Science and Technology Organization.*

References

Aizen V B, Aizen E M, Joswiak D R, Fujita K, Takeuchi N, Nikitin S A. 2006. Climatic and atmospheric circulation pattern variability from ice-core isotope/geochemistry records (Altai, Tien Shan and Tibet). Ann Glaciol, 43: 49–60

Balesdent J, Girardin C, Mariotti A. 1993. Site-related $\delta^{13}C$ of tree leaves and soil organic matter in a temperate forest. Ecology, 74: 1713–1721

Blaauw M, Christen J A. 2011. Flexible paleoclimate age-depth models using an autoregressive gamma process. Bayesian Anal, 6: 457–474

Böhner J. 2006. General climatic controls and topoclimatic variations in central and high Asia. Boreas, 35: 279–295

Buchmann N, Kao W Y, Ehleringer J. 1997. Influence of stand structure on carbon-13 of vegetation, soils, and canopy air within deciduous and evergreen forests in Utah, United States. Oecologia, 110: 109–119

Cai Y J, Chiang J H, Breitenbach S M, Tan L C, Cheng H, Edwards R L, An Z S. 2017. Holocene moisture changes in western China, Central Asia, inferred from stalagmites. Quat Sci Rev, 158: 15–28

Chen F H, Jia J, Chen J H, Li G Q, Zhang X J, Xie H C, Xia D S, Huang W, An C B. 2016. A persistent Holocene wetting trend in arid central Asia, with wettest conditions in the late Holocene, revealed by multi-proxy analyses of loess-paleosol sequences in Xinjiang, China. Quat Sci Rev, 146: 134–146

Chen F H, Yu Z C, Yang M L, Ito E, Wang S M, Madsen B D, Huang X Z, Zhao Y, Sato T, Birks J H, Boomer I, Chen J H, An C B, Wunnemann B. 2008. Holocene moisture evolution in arid central Asia and its out-of-phase relationship with Asian monsoon history. Quat Sci Rev, 27: 351–364

Chen T, Ma J, Feng H Y, He Y Q, Xu S J, Qiang W Y, An L Z. 2002. Environmental analysis of stable carbon isotope values in typical desert C_3 plants of the Fukang, Xinjiang. Arid Land Geogr, 25: 342–345

Cheng H, Zhang P Z, Spötl C, Edwards R L, Cai Y J, Zhang D Z, Sang W C, Tan M, An Z S. 2012. The climatic cyclicity in semiarid-arid central Asia over the past 500,000 years. Geophys Res Lett, 39: L01705

Deines P. 1980. The isotopic composition of reduced organic carbon. In: Fritz P, Fontes J C, eds. Handbook of Environmental Isotope Geochemistry I, The Terrestrial Environment. Amsterdam: Elsevier. 339–345

Dormoy I, Peyron O, Nebout N C, Goring S, Kotthoff U, Magny M, Pross J. 2009. Terrestrial climate variability and seasonality changes in the Mediterranean region between 15000 and 4000 years BP deduced from marine pollen records. Clim Past, 5: 615–632

Fang X M, Lu L Q, Yang S L, Li J J, An Z S, Jiang P G, Chen X L. 2002. Loess in Kunlun Mountains and its implications on desert development and Tibetan Plateau uplift in west China. Sci China Ser D-Earth Sci, 45:

289
Farquhar G D, Ehleringer J R, Hubick K T. 1989. Carbon isotope discrimination and photosynthesis. Annu Rev Plant Physiol Plant Mol Biol, 40: 503–537
Feng Y, Duan S M, Mu S Y, Zhao L, Zhao X H. 2012. Geographic distribution and ecology of C_4 plants in Xinjiang. Arid Land Geogr, 35: 145–153
Giresse P, Maley J, Brenac P. 1994. Late Quaternary palaeoenvironments in the Lake Barombi Mbo (West Cameroon) deduced from pollen and carbon isotopes of organic matter. Palaeogeogr Palaeoclimatol Palaeoecol, 107: 65–78
Gouveia S E M, Pessenda L C R, Aravena R, Boulet R, Scheel-Ybert R, Bendassoli J A, Ribeiro A S, Freitas H A. 2002. Carbon isotopes in charcoal and soils in studies of paleovegetation and climate changes during the late Pleistocene and the Holocene in the southeast and centerwest regions of Brazil. Glob Planet Change, 33: 95–106
Grootes P M, Stuiver M. 1997. Oxygen 18/16 variability in Greenland snow and ice with 10^3- to 10^5-year time resolution. J Geophys Res, 102: 26455–26470
Gu Z Y, Liu Q, Xu B, Han J M, Yang S L, Ding Z L, Liu D S. 2003. Climate as the dominant control on C_3 and C_4 plant abundance in the Loess Plateau: Organic carbon isotope evidence from the last glacial-interglacial loess-soil sequences. Chin Sci Bull, 48: 1271
Guo Z T, Ruddiman W F, Hao Q Z, Wu H B, Qiao Y S, Zhu R X, Peng S Z, Wei J J, Yuan B Y, Liu T S. 2002. Onset of Asian desertification by 22 Myr ago inferred from loess deposits in China. Nature, 416: 159–163
Haug G H, Ganopolski A, Sigman D M, Rosell-Mele A, Swann G E A, Tiedemann R, Jaccard S L, Bollmann J, Maslin M A, Leng M J, Eglinton G. 2005. North Pacific seasonality and the glaciation of North America 2.7 million years ago. Nature, 433: 821–825
He S L, Lu G H, Yang X D, Wang Y S, Liu X X, Yang J. 2010. Study on the main families and genera of vegetation in Aibi Lake wetland nature reserve using $\delta^{13}C_{org}$. Xinjiang Agr Sci, 47: 1421–1426
Hennissen J A I, Head M J, De Schepper S, Groeneveld J. 2015. Increased seasonality during the intensification of Northern Hemisphere glaciation at the Pliocene-Pleistocene boundary ~2.6 Ma. Quat Sci Rev, 129: 321–332
Herzschuh U. 2006. Palaeo-moisture evolution in monsoonal Central Asia during the last 50000 years. Quat Sci Rev, 25: 163–178
Hewitt C D, Mitchell J F B. 1996. Gcm simulations of the climate of 6 kyr BP: Mean changes and interdecadal variability. J Clim, 9: 3505–3529
Hong B, Gasse F, Uchida M, Hong Y T, Leng X T, Shibata Y, An N, Zhu Y X, Wang Y. 2014. Increasing summer rainfall in arid eastern-Central Asia over the past 8500 years. Sci Rep, 4: 5279
Huang X Z, Chen F H, Fan Y X, Yang M L. 2009. Dry late-glacial and early Holocene climate in arid Central Asia indicated by lithological and palynological evidence from Bosten Lake, China. Quat Int, 194: 19–27
Huang Y S, Street-Perrott F A, Metcalfe S E, Brenner M, Moreland M, Freeman K H. 2001. Climate change as the dominant control on glacial-interglacial variations in C_3 and C_4 plant abundance. Science, 293: 1647–1651
Kutzbach J E, Chen G, Cheng H, Edwards R L, Liu Z. 2013. Potential role of winter rainfall in explaining increased moisture in the Mediterranean and Middle East during periods of maximum orbitally-forced insolation seasonality. Clim Dyn, 42: 1079–1095
Lee X Q, Feng Z D, Guo L L, Wang L X, Jin L Y, Huang Y S, Chopping M, Huang D K, Jiang W, Jiang Q, Cheng H G. 2005. Carbon isotope of bulk organic matter: A proxy for precipitation in the arid and semiarid central East Asia. Glob Biogeochem Cycle, 19: GB4010
Li J F. 1991. Climate in Xinjiang. Beijing: China Meteorological Press. 74–124
Li X Q, Zhao K L, Dodson J, Zhou X Y. 2011. Moisture dynamics in central Asia for the last 15 kyr: New evidence from Yili Valley, Xinjiang, NW China. Quat Sci Rev, 30: 3457–3466
Liu W G, Huang Y S, An Z S, Clemens S C, Li L, Prell W L, Ning Y F. 2005a. Summer monsoon intensity controls C_4/C_3 plant abundance during the last 35 ka in the Chinese Loess Plateau: Carbon isotope evidence from bulk organic matter and individual leaf waxes. Palaeogeogr Palaeoclimatol Palaeoecol, 220: 243–254
Liu W G, Ning Y F, An Z S, Wu Z H, Lu H Y, Cao Y N. 2005b. Carbon isotopic composition of modern soil and paleosol as a response to vegetation change on the Chinese Loess Plateau. Sci China Ser D-Earth Sci, 48: 93–99
Liu W G, Li X Z, An Z S, Xu L M, Zhang Q L. 2013. Total organic carbon isotopes: A novel proxy of lake level from Lake Qinghai in the Qinghai-Tibet Plateau, China. Chem Geol, 347: 153–160
Liu W G, Liu Z H, An Z S, Sun J M, Chang H, Wang N, Dong J B, Wang H Y. 2014. Late Miocene episodic lakes in the arid Tarim Basin, western China. Proc Natl Acad Sci USA, 111: 16292–16296
Liu X Q, Herzschuh U, Shen J, Jiang Q F, Xiao X Y. 2008. Holocene environmental and climatic changes inferred from Wulungu Lake in northern Xinjiang, China. Quat Res, 70: 412–425
Long H, Shen J, Chen J H, Tsukamoto S, Yang L H, Cheng H Y, Frechen M. 2017. Holocene moisture variations over the arid central Asia revealed by a comprehensive sand-dune record from the central Tian Shan, NW China. Quat Sci Rev, 174: 13–32
Long H, Shen J, Tsukamoto S, Chen J H, Yang L H, Frechen M. 2014. Dry early Holocene revealed by sand dune accumulation chronology in Bayanbulak Basin (Xinjiang, NW China). Holocene, 24: 614–626
Lu H Y, Zhang H Y, Zeng L, Lu A Q, Zhang Z H, Chen Y Y, Yi S W. 2015. Temperature forced vegetation variations in glacial-interglacial cycles in northeastern China revealed by loess-laleosol deposit. Quat Sci, 35: 828–836
Luo C, Liu W G, Peng Z C, Yang D, He J F, Liu G J, Zhang P X. 2008. Stable carbon isotope record of organic matter from the Lop-nurl acustrine sediment in Xinjiang, northweat China. Quat Sci, 28: 621–628
Mackay A W, Bezrukova E V, Leng M J, Meaney M, Nunes A, Piotrowska N, Self A, Shchetnikov A, Shilland E, Tarasov P, Wang L, White D. 2012. Aquatic ecosystem responses to Holocene climate change and biome development in boreal, central Asia. Quat Sci Rev, 41: 119–131
Mathis M, Sorrel P, Klotz S, Huang X T, Oberhänsli H. 2014. Regional vegetation patterns at lake Son Kul reveal Holocene climatic variability in central Tien Shan (Kyrgyzstan, Central Asia). Quat Sci Rev, 89: 169–185
Meyers P A. 2003. Applications of organic geochemistry to paleolimnological reconstructions: A summary of examples from the Laurentian Great Lakes. Org Geochem, 34: 261–289
Meyers P A, Horie S. 1993. An organic carbon isotopic record of glacial-postglacial change in atmospheric pCO_2 in the sediments of Lake Biwa, Japan. Palaeogeogr Palaeoclimatol Palaeoecol, 105: 171–178
Meyers P A, Ishiwatari R. 1993. Lacustrine organic geochemistry—An overview of indicators of organic matter sources and diagenesis in lake sediments. Org Geochem, 20: 867–900
Meyers P A, Lallier-Vergés E. 1999. Lacustrine sedimentary organic matter records of Late Quaternary paleoclimates. J Paleolimnol, 21: 345–372
Monnin E, Indermühle A, Dällenbach A, Flückiger J, Stauffer B, Stocker T F, Raynaud D, Barnola J M. 2001. Atmospheric CO_2 concentrations over the last glacial termination. Science, 291: 112–114
Nordt L C, Boutton T W, Jacob J S, Mandel R D. 2002. C_4 plant productivity and climate-CO_2 variations in South-Central Texas during the Late Quaternary. Quat Res, 58: 182–188
O'Leary M H. 1981. Carbon isotope fractionation in plants. Phytochemistry, 20: 553–567
O'Leary M H. 1988. Carbon isotope in photosynthesis. BioScience, 38: 328–336
Petit J R, Jouzel J, Raynaud D, Barkov N I, Barnola J M, Basile I, Bender M, Chappellaz J, Davis M, Delaygue G, Delmotte M, Kotlyakov V M, Legrand M, Lipenkov V Y, Lorius C, PÉpin L, Ritz C, Saltzman E, Stievenard M. 1999. Climate and atmospheric history of the past 420000 years from the Vostok ice core, Antarctica. Nature, 399: 429–436
Peyron O, Goring S, Dormoy I, Kotthoff U, Pross J, de Beaulieu J L, Drescher-Schneider R, Vannière B, Magny M. 2011. Holocene sea-

sonality changes in the central Mediterranean region reconstructed from the pollen sequences of Lake Accesa (Italy) and Tenaghi Philippon (Greece). Holocene, 21: 131–146

Ran M, Feng Z D. 2014. Variation in carbon isotopic composition over the past ca. 46000 yr in the loess-paleosol sequence in central Kazakhstan and paleoclimatic significance. Org Geochem, 73: 47–55

Rao Z G, Xu Y B, Xia D S, Xie L H, Chen F H. 2013. Variation and paleoclimatic significance of organic carbon isotopes of Ili loess in arid Central Asia. Org Geochem, 63: 56–63

Rao Z G, Chen F H, Cheng H, Liu W G, Wang G A, Lai Z P, Blomental J. 2013. High-resolution summer precipitation variations in the western Chinese Loess Plateau during the last glacial. Sci Rep, 3: 2785

Rea D K, Snoeckx H, Joseph L H. 1998. Late Cenozoic eolian deposition in the North Pacific: Asian drying, Tibetan uplift, and cooling of the northern hemisphere. Paleoceanography, 13: 215–224

Reimer P J, Bard E, Bayliss A, Beck J W, Blackwell P G, Ramsey C B, Buck C E, Cheng H, Edwards R L, Friedrich M, Grootes P M, Guilderson T P, Haflidason H, Hajdas I, Hatté C, Heaton T J, Hoffmann D L, Hogg A G, Hughen K A, Kaiser K F, Kromer B, Manning S W, Niu M, Reimer R W, Richards D A, Scott E M, Southon J R, Staff R A, Turney C S M, van der Plicht J. 2013. IntCal13 and Marine13 radiocarbon age calibration curves 0–50000 years cal BP. Radiocarbon, 55: 1869–1887

Rudaya N, Li H C. 2013. A new approach for reconstruction of the Holocene climate in the Mongolian Altai: The high-resolution $\delta^{13}C$ records of TOC and pollen complexes in Hoton-Nur Lake sediments. J Asian Earth Sci, 69: 185–195

Rudaya N, Tarasov P, Dorofeyuk N, Solovieva N, Kalugin I, Andreev A, Daryin A, Diekmann B, Riedel F, Tserendash N, Wagner M. 2009. Holocene environments and climate in the Mongolian Altai reconstructed from the Hoton-Nur pollen and diatom records: A step towards better understanding climate dynamics in Central Asia. Quat Sci Rev, 28: 540–554

Sage R F, Wedin D A, Li M. 1999. The biogeography of C_4 photosynthesis: Patterns and controlling factors. In: Sage R F, Monson R K, eds. C_4 Plant Biology. San Diego: Academic Press. 313–373

Schubert B A, Jahren A H. 2012. The effect of atmospheric CO_2 concentration on carbon isotope fractionation in C_3 land plants. Geochim Cosmochim Acta, 96: 29–43

Shen J, Wang S M, Zhang G. 1998a. Dissolvable organic composition and its paleoclimatte and enviromental significance in sediments of Gucheng Lake. J Lake Sci, 10: 63–70

Shen J, Wu R J, An Z S. 1998b. Characters of the organic $\delta^{13}C$ and paleoenvironment in the section of Dubusu Lake. J Lake Sci, 10: 8–12

Song Y G, Shi Z T, Fang X M, Nie J S, Naoto I, Qiang X K, Wang X L. 2010. Loess magnetic properties in the Ili Basin and their correlation with the Chinese Loess Plateau. Sci China Earth Sci, 53: 419–431

Stuiver M, Grootes P M, Braziunas T F. 1995. The GISP2 $\delta^{18}O$ climate record of the past 16,500 years and the role of the sun, ocean, and volcanoes. Quat Res, 44: 341–354

Sun B Y, Yue L P, Lai Z P, Liu W G. 2014. Paleoclimate change recorded by sediment organic carbon isotope of Lake Barkol since 14 ka BP. Quat Sci, 34: 418–424

Sun H L, Ma J Y, Wang S M, Zhang X. 2007. The study of stable carbon isotope composition in desert plants of Junggar Basin. J Desert Res, 27: 972–976

Sun J M, Ye J, Wu W Y, Ni X J, Bi S D, Zhang Z Q, Liu W M, Meng J. 2010. Late Oligocene-Miocene mid-latitude aridification and wind patterns in the Asian interior. Geology, 38: 515–518

Sun X J, Du N Q, Weng C Y, Lin R F, Wei K Q. 1994. Paleovegetation and paleoenvironment of Manas Lake, Xinjiang, Northwestern China during the last 14000 years. Quat Sci, 3: 239–248

Wang G A, Feng X, Han J M, Zhou L P, Tan W, Su F. 2008. Paleovegetation reconstruction using $\delta^{13}C$ of Soil Organic Matter. Biogeosciences, 5: 1325–1337

Wang G A, Li J Z, Liu X Z, Li X Y. 2013. Variations in carbon isotope ratios of plants across a temperature gradient along the 400 mm isoline of mean annual precipitation in north China and their relevance to paleovegetation reconstruction. Quat Sci Rev, 63: 83–90

Wang G A, Zhang L L, Zhang X Y, Wang Y H, Xu Y P. 2014. Chemical and carbon isotopic dynamics of grass organic matter during litter decompositions: A litterbag experiment. Org Geochem, 69: 106–113

Wang Y, Zhu L P, Wang J B, Ju J T, Lin X. 2012. The spatial distribution and sedimentary processes of organic matter in surface sediments of Nam Co, Central Tibetan Plateau. Chin Sci Bull, 57: 4753–4764

Woszczyk M, Bechtel A, Gratzer R, Kotarba M J, Kokociński M, Fiebig J, Cieśliński R. 2011. Composition and origin of organic matter in surface sediments of Lake Sarbsko: A highly eutrophic and shallow coastal lake (northern Poland). Org Geochem, 42: 1025–1038

Wynn J G. 2007. Carbon isotope fractionation during decomposition of organic matter in soils and paleosols: Implications for paleoecological interpretations of paleosols. Palaeogeogr Palaeoclimatol Palaeoecol, 251: 437–448

Xinjiang Expedition Team, Chinese Academy of Sciences. 1978. Vegetation and its Utilization in Xinjiang. Beijing: Sciences Press. 1–266

Yang S L, Ding Z L. 2006. Winter-spring precipitation as the principal control on predominance of C_3 plants in Central Asia over the past 1.77 Myr: Evidence from $\delta^{13}C$ of loess organic matter in Tajikistan. Palaeogeogr Palaeoclimatol Palaeoecol, 235: 330–339

Yang S L, Ding Z L, Li Y Y, Wang X, Jiang W Y, Huang X F. 2015. Warming-induced northwestward migration of the East Asian monsoon rain belt from the Last Glacial Maximum to the mid-Holocene. Proc Natl Acad Sci USA, 112: 13178–13183

Yang X P, Zhu Z D, Jaekel D, Owen L A, Han J M. 2002. Late Quaternary palaeoenvironment change and landscape evolution along the Keriya River, Xinjiang, China: The relationship between high mountain glaciation and landscape evolution in foreland desert regions. Quat Int, 97-98: 155–166

Ye W. 1999. Characteristics of physical environment and conditions of loess formation in Yili area, Xijing. Arid Land Geogr, 22: 9–16

Zhang Y, Meyers P A, Liu X T, Wang G P, Ma X H, Li X Y, Yuan Y X, Wen B L. 2016. Holocene climate changes in the central Asia mountain region inferred from a peat sequence from the Altai Mountains, Xinjiang, northwestern China. Quat Sci Rev, 152: 19–30

Zhao K L, Li X Q, Dodson J, Zhou X Y, Atahanc P. 2013. Climate instability during the last deglaciation in central Asia, reconstructed by pollen data from Yili Valley, NW China. Rev Palaeobot Palynol, 189: 8–17

Zhao Y, Liu Y L, Guo Z T, Fang K Y, Li Q, Cao X Y. 2017. Abrupt vegetation shifts caused by gradual climate changes in central Asia during the Holocene. Sci China Earth Sci, 60: 1317–1327

Zheng H B, Wei X C, Tada R, Clift P D, Wang B, Jourdan F, Wang P, He M Y. 2015. Late Oligocene-early Miocene birth of the Taklimakan Desert. Proc Natl Acad Sci USA, 112: 7662–7667

(Responsible editor: Yan ZHAO)